Journal of Applied Geophysics 137 (2017) 49–54

Contents lists available at ScienceDirect

Journal of Applied Geophysics

journal homepage: www.elsevier.com/locate/jappgeo

Rapid simulation of electromagnetic telemetry using an axisymmetric semianalytical finite element method

Jiefu Chen[a], Shubin Zeng[a], Qiuzhao Dong[b], Yueqin Huang[c,*]

[a] University of Houston, United States
[b] Weatherford International, United States
[c] Cyentech Consulting LLC, United States

ARTICLE INFO

Article history:
Received 17 July 2016
Received in revised form 29 November 2016
Accepted 5 December 2016
Available online 7 December 2016

Keywords:
Electromagnetic telemetry
Measurement-while-drilling
Semianalytical finite element method
High precision integration
Layered media

ABSTRACT

An axisymmetric semianalytical finite element method is proposed and employed for rapid simulations of electromagnetic telemetry in layered underground formation. In this method, the layered media is decomposed into several subdomains and the interfaces between subdomains are discretized by conventional finite elements. Then a Riccati equation based high precision integration scheme is applied to exploit the homogeneity along the vertical direction in each layer. This semianalytical finite element scheme is very efficient in modeling electromagnetic telemetry in layered formation. Numerical examples as well as a field case with water based mud as drilling fluid are given to demonstrate the validity and effectiveness of this method.

1. Introduction

Telemetry is a wireless and real-time technique for borehole communication between surface and downhole sensors in exploration of underground resources, such as oil and gas, mineral, and geothermal. The most commonly used telemetry techniques in measurement-while-drilling (MWD) and logging-while-drilling (LWD) systems are mud pulse telemetry and electromagnetic telemetry. For mud pulse telemetry, a downhole valve is operated to restrict the flow of drilling mud and to create pressure pulse carrying digital information and propagating to the surface. Because of the dependence on consistent wellbore hydraulics, mud pulse telemetry cannot work in underbalanced drilling with air, mist, or foam. Electromagnetic telemetry is based on the propagation of electromagnetic waves between bottom hole assembly (BHA) and the surface. It is a reliable method providing borehole communication in underbalanced drilling. On the other hand, electromagnetic telemetry suffers severe signal attenuation when conductive formation layers exist between transmitter and receiver. Therefore, accurate and efficient modeling turns out to be indispensable in designing and optimizing an electromagnetic telemetry system, evaluating the feasibility for each field job, and guiding a successful deployment for a specific well configuration.

Both approximate analysis based on some kind of simplified model and rigorous numerical methods have been used for EM telemetry modeling. The attenuation prediction method proposed by Soulier et al. (1993) approximates the electromagnetic transmission channel as a ladder network with a coaxial cable. It considers the drill string and the casing as the central conductor and the formations situated at the infinity as the external conductor. Underground formation are treated as non-perfect insulation between the two conductors. Then a simplified mathematical model is applied by representing the coaxial cable as a series of cells containing two impedance in an L-shaped configuration and the total attenuation is the summation of successive attenuations produced by each cell (Maglione et al., 1994). This method is very fast but with significant inaccuracies due to the poor approximation of true formation properties with complex distribution, the coarse correction factor based on experience, and the lack of frequency independency in the model. In the work by DeGauque et al. (1987) the electromagnetic telemetry system is approximated as a quasi-static problem in a homogeneous formation, and this simplified model is solved as a thin wire by method of moments (MoM). This work suggests that the attenuation of telemetry signal will be a constant below some given frequency and decreasing the operating frequency will not increase the communication range. Xia and Chen (1993) examined the attenuation of electromagnetic telemetry signal by assuming that the drill string is a perfect conductor, the formation is homogeneous and the influence of the mud column is negligible. Later, Trofimenkoff et al. (2000)

* Corresponding author.

http://dx.doi.org/10.1016/j.jappgeo.2016.12.006
0009-2541/

took the electrical properties of the drill pipe, joint resistance, voltage source resistance and earth propagation effects into account and used the method of images to solve the channel attenuation of the DC model described as a ladder network problem. Similar to Trofimenkoff's method, Carcione and Poletto (2002) described the system by telegrapher equations with frequency dependency taken into account.

For rigorous modeling of an electromagnetic telemetry system in a complicated environment, numerical methods such as finite element method (FEM) becomes a necessity. FEM can take all the features in an electromagnetic telemetry system such as drill pipes, drilling fluid in the borehole, multiple layers of casing and cement, and earth formation into consideration. However, the efficiency of conventional FEM method will be rather low when used to model a deep well, or when the number of underground layers is large. Vong et al. (2005) used a hybrid of axisymmetric finite elements and surface impedance method to accelerate the computing speed. The drill pipe, casing, drill bit, and other parts are modeled by conventional FEM elements. The large region of conducting media surrounding the drill string is approximately taken into account using a surface impedance technique. In this paper, we introduce the recently developed semianalytical finite element method (Chen, 2015b, Chen et al., 2011b) to solve axisymmetric electromagnetic problems, and apply it for simulations of electromagnetic telemetry systems in vertical wells. The steps are as follows: firstly, a layered structure is decomposed into several subdomains, within each one the geometry and material distribution are homogeneous in the vertical direction; secondly, the conventional 1D finite elements are used to discretize the cross section of each layer; thirdly, a Riccati equation based integration scheme is employed to perform the vertical integration with a very high level of accuracy. Several numerical examples are given to demonstrate the high levels of efficiency and accuracy of this semianalytical finite element method, and to analyze the performance of the electromagnetic telemetry system with respect to various system parameters. A field case will also be given to demonstrate the validity of the proposed method in real situations.

2. Problem statement

Fig. 1 shows a schematic of an electromagnetic telemetry system. A transmitter in this wireless communication system is near the drill bit implemented as a voltage gap source or a toroid, which

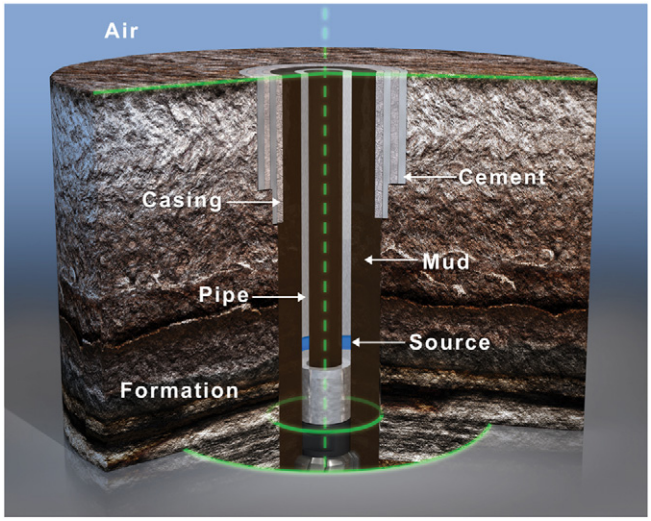

Fig. 1. A schematic of electromagnetic telemetry.

can be viewed as an electric dipole or as a magnetic current source circulating the drill string in analysis. A receiver is set on the surface with two terminals: one is attached to the blowout preventer (BOP), and the other one is connected to an earth antenna as a metal stake driven into the ground with a certain distance away from the rig. In a two-way telemetry system the surface antenna will be set as transmitter, and the one in downhole will be used to pick up commands sent from surface. The performance of an electromagnetic telemetry system is strongly affected by properties of the underground formation, which oftentimes is treated as a layered structure along the vertical direction. On the other hand, the telemetry system in a vertical well can also be treated as a cylindrically layered structure: several layers including steel drill string, drilling fluid in the borehole, casing, cement, and formation can be found from the center of wellbore to outside along the radial direction. Such a doubly layered structure with a loop of magnetic current as the source will be an axisymmetric and transverse magnetic (TM) problem. The corresponding governing equation with variable H_ϕ is

$$\frac{\partial}{\partial\rho}\left(\frac{1}{\rho\hat{\epsilon}_r}\frac{\partial}{\partial\rho}(\rho H_\phi)\right)+\frac{\partial}{\partial z}\left(\frac{1}{\hat{\epsilon}_r}\frac{\partial H_\phi}{\partial z}\right)+k_0^2\mu_r H_\phi = j\frac{k_0}{Z_0}M_\phi \tag{1}$$

where k_0 and Z_0 denote wavenumber and intrinsic impedance of the free space, respectively. μ_r is the relative permeability. Complex relative permittivity $\hat{\epsilon}_r = \epsilon_r - j\sigma/(\omega\epsilon_0)$. ϵ_0 is permittivity of vacuum. ϵ_r and σ are relative permittivity and conductivity, respectively. There are two ways of implementing a downhole source: for voltage source, magnetic current M_ϕ circulating the drill string needs to be specified at the source position; for current source, the magnitude of current flowing along the pipe needs to be known, which is equivalent to the Dirichlet boundary condition for magnetic field at the source position. These two types of source implementation are equivalent to each other based on normalized output power, i.e., the multiplication of voltage jump at the source (known for the first implementation, and to be calculated for the second implementation) and current flow at the source (known for the second implementation, and to be calculated for the first implementation).

M_ϕ is imposed magnetic current density circulating the drill string. The functional corresponding to Eq. (1) is

$$\begin{aligned}\Pi(H_\phi) =& \pi\int_{z_a}^{z_b}\int_{\rho_a}^{\rho_b}\left[\frac{1}{\hat{\epsilon}_r}\left(\frac{1}{\rho}\frac{\partial}{\partial\rho}(\rho H_\phi)\right)^2+\frac{1}{\hat{\epsilon}_r}\left(\frac{\partial H_\phi}{\partial z}\right)^2\right]\rho d\rho dz\\ &-\pi\int_{z_a}^{z_b}\int_{\rho_a}^{\rho_b}k_0^2\mu_r H_\phi^2\rho d\rho dz+2\pi\int_{z_a}^{z_b}\int_{\rho_a}^{\rho_b}j\frac{k_0}{Z_0}M_\phi H_\phi\rho d\rho dz\end{aligned} \tag{2}$$

where z_a, z_b, ρ_a, and ρ_b define the computational domain of the axisymmetric problem in the cylindrical system. Define $J = 2\pi\rho H_\phi$ as current flowing along drill string, the functional based on the new variable is

$$\begin{aligned}\Pi(J) =& \frac{1}{4\pi}\int_{z_a}^{z_b}\int_{\rho_a}^{\rho_b}\left[\frac{1}{\rho\hat{\epsilon}_r}\left(\frac{\partial J}{\partial\rho}\right)^2+\frac{1}{\rho\hat{\epsilon}_r}\left(\frac{\partial J}{\partial z}\right)^2\right]d\rho dz\\ &-\frac{1}{4\pi}\int_{z_a}^{z_b}\int_{\rho_a}^{\rho_b}\frac{1}{\rho}k_0^2\mu_r J^2 d\rho dz+\int_{z_a}^{z_b}\int_{\rho_a}^{\rho_b}j\frac{k_0}{Z_0}M_\phi J d\rho dz\end{aligned} \tag{3}$$

The above functional can be discretized and solved by conventional 2D finite elements. However, the efficiency may become rather low if the computational domain becomes very large (e.g. deep well), or the number of formation layers is large. In this paper we will use a recently developed semianalytical finite element method (Chen, 2015b; Chen et al., 2011b) to solve this axisymmetric electromagnetic problem. Based on the geometric characteristics of the telemetry system, the computational domain will be decomposed

into a set of layers, and the structure of each layer is uniform along the vertical direction. 1D finite elements are employed for the discretization of cross section, while the vertical direction is left as undiscretized and will be handled by a Riccati equation based integration scheme (Zhong, 2004) with a very high level of accuracy regardless of the thickness of the layer. By transforming this 2D axisymmetric simulation into a set of 1D FEM discretization, the proposed method will lead to much less unknowns and higher efficiency compared with conventional FEM.

3. Axisymmetric semianalytical finite element method

Assigning separating planes at the interfaces between layers and at the locations where excitations are imposed, the computational domain will be decomposed into subdomains uniform along the vertical direction. Use 1D finite element for the cross section of a layer and leave the vertical direction untouched, the volume integration part of functional Eq. (3) will be

$$\Pi(\mathbf{I}) = \frac{1}{2}\int_{z_a}^{z_b}\left(\mathbf{J}^T\mathbf{K}_1\mathbf{J} + \dot{\mathbf{J}}^T\mathbf{K}_2\dot{\mathbf{J}}\right)dz \tag{4}$$

where $\dot{\mathbf{J}} = \frac{\partial \mathbf{J}}{\partial z}$, and

$$\mathbf{K}_1 = \sum_e \int_{z_a}^{z_b}\left(\frac{1}{2\pi\rho\hat{\epsilon}_r}\frac{\partial \mathbf{N}_e}{\partial \rho}\cdot\frac{\partial \mathbf{N}_e^T}{\partial \rho} - \frac{k_0^2\mu_r}{2\pi\rho}\mathbf{N}_e\cdot\mathbf{N}_e^T\right)dz \tag{5}$$

$$\mathbf{K}_2 = \sum_e \int_{z_a}^{z_b}\left(\frac{1}{2\pi\rho\hat{\epsilon}_r}\mathbf{N}_e\cdot\mathbf{N}_e^T\right)dz \tag{6}$$

$\mathbf{N}_e$ for the e-th element is a vector containing basis functions as well as testing functions, which can be any 1D interpolatory functions. For example, linear basis functions are used in the numerical examples in this paper. Carrying out integration w.r.t. z in the semi-discretized functional Eq. (4), we will obtain a fully discretized functional as a quadratic function of $\mathbf{J}_a = \mathbf{J}|_{z=z_a}$ and $\mathbf{J}_b = \mathbf{J}|_{z=z_b}$, the values of discretized $\mathbf{J}$ on the upper and lower boundaries of a layer.

$$\Pi(\mathbf{J}_a,\mathbf{J}_b) = \frac{1}{2}\mathbf{J}_a^T\mathbf{K}_{aa}\,\mathbf{J}_a + \mathbf{J}_b^T\mathbf{K}_{ba}\,\mathbf{J}_a + \frac{1}{2}\mathbf{J}_b^T\mathbf{K}_{bb}\,\mathbf{J}_b \tag{7}$$

Matrices $\mathbf{K}_{aa}$, $\mathbf{K}_{ba}$ can be obtained by applying some numerical integration technique to functional Eq. (4) w.r.t. the z direction. However, doing this way the accuracy cannot be guaranteed and we lose the chance of exploiting the uniform structural distribution of the layer in the vertical direction. A Riccati equation based high precision integration method (Zhong, 2004) can be employed here to deal with the vertical integration with a very high level of accuracy.

It have been proven (Zhong, 2006) that system matrices $\mathbf{K}_{aa}$, $\mathbf{K}_{ba}$, and $\mathbf{K}_{bb}$ can be obtained from

$$\begin{cases}\mathbf{K}_{aa} = -\mathbf{Q} + \mathbf{F}^T\mathbf{G}^{-1}\mathbf{F}\\ \mathbf{K}_{ba} = -\mathbf{G}^{-1}\mathbf{F}\\ \mathbf{K}_{bb} = \mathbf{G}^{-1}\end{cases} \tag{8}$$

And the three matrices $\mathbf{Q}$, $\mathbf{F}$ and $\mathbf{G}$ are solutions to a set of Riccati equations

$$\begin{cases} d\mathbf{F}/d\eta = -\mathbf{G}\mathbf{K}_1\mathbf{F} = \mathbf{F}\mathbf{K}_2^{-1}\mathbf{Q}\\ d\mathbf{G}/d\eta = \mathbf{K}_2^{-1} - \mathbf{G}\mathbf{K}_1\mathbf{G} = \mathbf{F}\mathbf{K}_2^{-1}\mathbf{F}^T\\ d\mathbf{Q}/d\eta = -\mathbf{F}\mathbf{K}_1\mathbf{F} = \mathbf{Q}\mathbf{K}_2^{-1}\mathbf{Q} - \mathbf{K}_1\end{cases} \tag{9}$$

with initial conditions

$$\begin{cases}\mathbf{Q}|_{\eta\to 0} = \mathbf{0}\\ \mathbf{G}|_{\eta\to 0} = \mathbf{0}\\ \mathbf{F}|_{\eta\to 0} = \mathbf{I}\end{cases} \tag{10}$$

where $\eta = z_b - z_a$ is the thickness of the layer. $\mathbf{0}$ is a zero matrix, and $\mathbf{I}$ is an identity matrix with the same dimension of $\mathbf{K}_1$ or $\mathbf{K}_2$.

A high precision integration scheme (Zhong, 2004) has been developed to solve the above Riccati equations with relative errors as small as machine epsilon on a computer. The first step in this scheme is to divide the integration interval η into 2^N slices

$$\tau = \frac{\eta}{2^N} \tag{11}$$

where N is a positive integer number. Under most circumstances, choosing $N = 20$ will make the integration error comparable to machine epsilon defined by double precision. $N = 20$ means $\tau = \eta/1,048,576$, i.e., even for a layer as thick as 1000 wavelengths, a slice with value τ will be thinner than $1/1000$ of a wavelength. It is sufficient to use Taylor expansion to calculate matrices $\mathbf{F}$, $\mathbf{G}$, $\mathbf{Q}$ within the small interval τ

$$\begin{cases}\mathbf{F}(\tau) = \mathbf{I} + \mathbf{F}'(\tau)\\ \mathbf{F}'(\tau) = \phi_1\tau + \phi_2\tau^2 + \phi_3\tau^3 + \phi_4\tau^4 + O(\tau^5)\\ \mathbf{G}(\tau) = \gamma_1\tau + \gamma_2\tau^2 + \gamma_3\tau^3 + \gamma_4\tau^4 + O(\tau^5)\\ \mathbf{Q}(\tau) = \theta_1\tau + \theta_2\tau^2 + \theta_3\tau^3 + \theta_4\tau^4 + O(\tau^5)\end{cases} \tag{12}$$

where ϕ, γ, θ are matrices with the same dimensions as $\mathbf{F}$, $\mathbf{G}$, $\mathbf{Q}$. Because τ is a very small number, the higher order items $O(\tau^5)$ by Taylor expansion will be smaller than or comparable to machine epsilon on a computer, and dropping off these higher order items will not lead to the loss of any significant digits. A comparison between Eqs. (12) and (9) will give expressions of ϕ, γ, θ:

$$\begin{cases}\gamma_1 = \mathbf{K}_2^{-1}\\ \gamma_2 = \mathbf{0}\\ \gamma_3 = -\gamma_1\mathbf{K}_1\gamma_1/3\\ \gamma_4 = \mathbf{0}\end{cases} \tag{13}$$

$$\begin{cases}\phi_1 = \mathbf{0}\\ \phi_2 = -\gamma_1\mathbf{K}_1/2\\ \phi_3 = \mathbf{0}\\ \phi_4 = \left(-\gamma_3\mathbf{K}_1 - \gamma_1\mathbf{K}_1\phi_2\right)/4\end{cases} \tag{14}$$

$$\begin{cases}\theta_1 = -\mathbf{K}_1\\ \theta_2 = \mathbf{0}\\ \theta_3 = \left(-\phi_2\mathbf{K}_1 - \mathbf{K}_1\phi_2\right)/3\\ \theta_4 = \mathbf{0}\end{cases} \tag{15}$$

And the solutions of three matrices over interval 2τ, i.e. $\mathbf{F}(2\tau)$, $\mathbf{G}(2\tau)$, $\mathbf{Q}(2\tau)$ will be

$$\begin{cases}\mathbf{G}(2\tau) = \mathbf{G}(\tau) + \mathbf{F}(\tau)[\mathbf{G}(\tau)^{-1} + \mathbf{Q}(\tau)]^{-1}\mathbf{F}(\tau)^T\\ \mathbf{F}'(2\tau) = \mathbf{F}'(\tau)[\mathbf{I} + \mathbf{G}(\tau)\mathbf{Q}(\tau)]^{-1}\mathbf{F}'(\tau)\\ \qquad\qquad +[(\mathbf{F}'(\tau) - \mathbf{G}(\tau)\mathbf{Q}(\tau)/2][\mathbf{I} + \mathbf{G}(\tau)\mathbf{Q}(\tau)]^{-1}\\ \qquad\qquad +[\mathbf{I} + \mathbf{G}(\tau)\mathbf{Q}(\tau)]^{-1}[\mathbf{F}'(\tau) - \mathbf{G}(\tau)\mathbf{Q}(\tau)/2]\\ \mathbf{Q}(2\tau) = \mathbf{Q}(\tau) + \mathbf{F}(\tau)^T[\mathbf{Q}(\tau)^{-1} + \mathbf{G}(\tau)]^{-1}\mathbf{F}(\tau)\end{cases} \tag{16}$$

It should be noted that only the increment $\mathbf{F}'(\tau) = \mathbf{F}(\tau) - \mathbf{I}$ instead of $\mathbf{F}(\tau)$ itself is calculated and stored during the above step. The reason that the small quantity must be kept away from $\mathbf{I}$ during computation, otherwise significant digits of $\mathbf{F}'(\tau)$ will be lost if add a small quantity $\mathbf{F}'(\tau)$ to a much larger quantity $\mathbf{I}$. Repeating Eq. (16) for N times, the integration interval will grow to η, and we then can obtain the matrices $\mathbf{G}(\eta)$, $\mathbf{Q}(\eta)$, and $\mathbf{F}(\tau) = \mathbf{F}'(\tau) + \mathbf{I}$ with a very high level of

Table 1
Relative error of high precision integration w.r.t. different value of N.

Value of N	Integration points (2^N)	Relative error
2	4	2.7776e−01
4	16	1.2431e−03
6	64	4.8636e−06
8	256	1.9000e−08
10	1024	7.4220e−11
12	4096	2.9019e−13
14	16,384	6.4325e−16
16	65,536	2.4493e−16
18	262,144	2.0213e−15
20	1,048,576	2.4493e−16

accuracy. Table 1 lists relative errors of the high precision integration for a simple case as a plane wave traveling through a distance of one wavelength in a homogeneous medium. We can see that when N is equal to or larger than 14, the relative error is close to 2.22×10^{-16}, which is the machine epsilon defined by double precision. This table suggests that to achieve a higher accuracy or efficiency, N in the proposed algorithm can be chosen adaptively based on the thickness of each layer along the z direction, instead of being fixed as $N = 20$.

After performing the high precision integration in the vertical direction, the final system matrix of this layer will be as

$$\mathbf{K}_e = \begin{bmatrix} \mathbf{K}_{aa} & \mathbf{K}_{ba}^T \\ \mathbf{K}_{ba} & \mathbf{K}_{bb} \end{bmatrix} \tag{17}$$

At this stage this discretized layers is ready to be assembled with adjacent layers, discretized by either conventional finite elements or by the proposed semianalytical elements. After the global system matrix is formed, and the sources terms is assigned to the right hand sides, numerical results will be obtained by solving the system of equations and based on which the performance of the electromagnetic telemetry system can be evaluated. Oftentimes the formation for EM telemetry study can be regarded as a layered earth model based on resistivity log. The system matrix by the semianalytical FEM for a layered structure will be in a block tridiagonal form (Chen, 2015a), which can be efficiently solved by the block Thomas algorithm (Chen et al., 2011a, Meurant, 1992) with the computational cost linearly proportional to the number of layers. The combination of semianalytical FEM with the block Thomas algorithm is promising in modeling EM telemetry in unground formation with a large number of layers.

4. Numerical examples

We first consider a well in a homogeneous underground formation with resistivity 1 ohm-m. The total length of the drill string is 5000 ft. The diameters of the drill pipe and the borehole are 10 in. and 12 in., respectively. The length of casing string as well as the cement is 3000 ft. The resistivity of drilling fluid filled in borehole is set as 1 ohm-m. The conductivities of both drilling pipe and casing string are assumed as 2e6 S/m. The downhole transmitter as a constant 1 V voltage source is 200 ft behind the drill bit transmitting signals at 5 Hz working frequency, and the surface receiver is measuring the voltage difference between the BOP and a point 500 ft away from the rig. Fig. 2 shows the calculated amplitude of current flowing along the drill string. We can see that the amplitude of current gradually decreases as it is away from the source, and this is because part of current is injected into conductive formation while flowing along the drill string. From this figure we can also observe that the current magnitude deceases faster since the since the depth of 3000 ft and upwardly, and this is due to the existence of steel casing. The current flow along the drill pipe calculated by both conventional FEM and the proposed semianalytical FEM are shown in

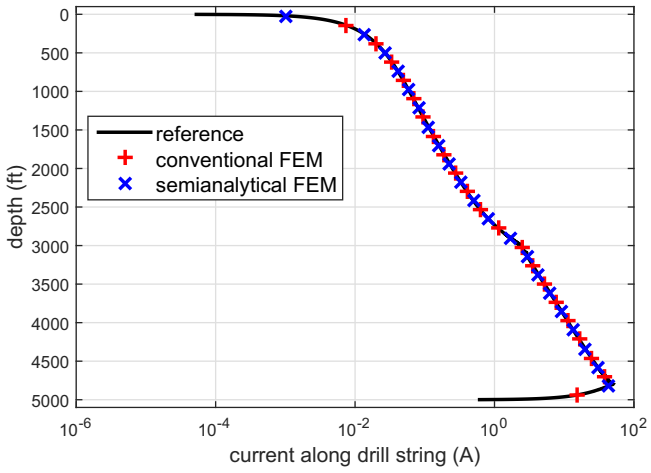

Fig. 2. Amplitude of current flow along the drill string in a homogeneous formation model.

Fig. 2. This figure also shows the reference results, which is obtained by conventional FEM with a very fine mesh. We can see that the results by both numerical schemes agree well with the reference. A quantitative comparison between the two schemes suggests that to achieve a similar level of accuracy (in this case relative errors are 9.71e−3 and 7.46e−3 for conventional FEM and semianalytical FEM, respectively), the semianalytical FEM costs much less computational time (34.57 s) than does the conventional FEM (302.10 s). A laptop with an Intel Core i7-4600U CPU at 2.1 GHz and 16 GB memory was used in this case and all the following examples.

Table 2 lists the computational costs of electromagnetic telemetry systems for wells with different depth by the two numerical schemes. We can see that the computational cost by the conventional FEM increases rapidly as the well goes deeper. This is because a deeper well means a larger domain of simulation, and consequently more elements in discretization as well as a larger system of equations to solve. On the other hand, the computational time by the semianalytical FEM stays about the same regardless of the depth of the well. The reason is that semianalytical FEM only requires discretization on the cross section of each layer, and this scheme can handle the vertical integration very accurately no matter how thin or how thick the layer is.

The three most significant factors deciding the EM telemetry signal strength are working frequency, resistivity or conductivity of underground formation, and drilling depth. Fig. 3 shows simulated results of the signal strength of an electromagnetic telemetry signal w.r.t. different system parameters. We can see that the strength of telemetry signal decreases rapidly as the drilling goes deeper or formation becomes more conductive, or if a higher working frequency is employed for faster data transmission. In this figure we also notice that all the curves become saturated in the high resistivity region, and the reason is the downhole source reaches the voltage

Table 2
Number of finite elements in discretization, and simulation time of electromagnetic telemetry systems with different depth by conventional FEM (scheme 1) and the semianalytical FEM (scheme 2).

Depth of drill bit	Scheme 1	Scheme 1	Scheme 2	Scheme 2
	# of elements	CPU time	# of elements	CPU time
2000 ft	130,048	59.21 s	320	33.97 s
4000 ft	236,966	233.64 s	320	33.84 s
6000 ft	340,154	353.32 s	320	35.09 s
8000 ft	539,963	787.50 s	320	34.63 s
10,000 ft	667,234	1259.93 s	320	35.11 s

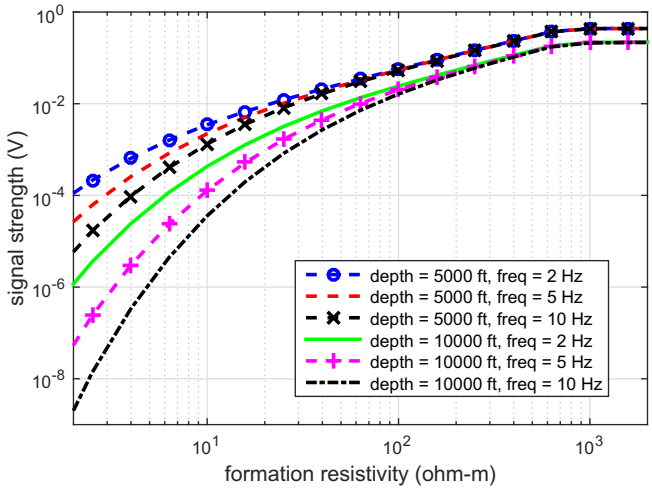

Fig. 3. Telemetry signals with different working frequency, drilling depth, and formation resistivity.

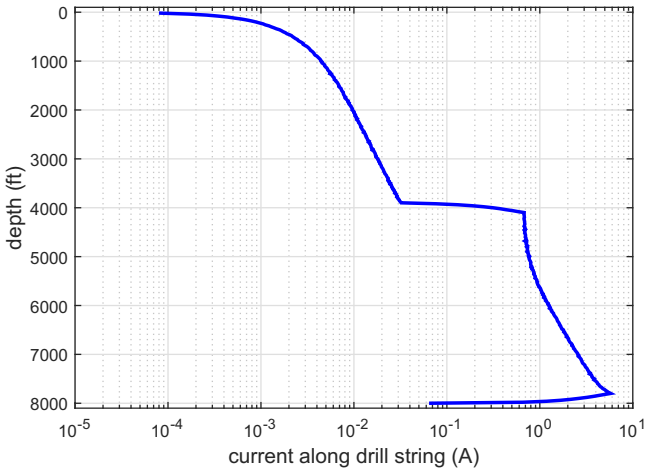

Fig. 5. Amplitude of current flow along the drill string in a layered formation model.

limit when it is located in a highly resistive formation. Fig. 4 shows the output voltage of a constant current downhole source against different formation resistivity, and the maximum output voltage is assumed as 18 V in this case (without considering the upper limit of output power in this case). From this figure we can see that the higher the level of constant current the downhole source uses, the lower the formation resistivity for the source to turn saturated. In other words, a lower level of output current should be chosen if the drill bit is in a highly resistive formation. Besides of the three aforementioned factors, the type of drilling fluid will also greatly affect the performance of an EM telemetry system. Previous studies (Soulier et al., 1993) and field experiences suggest that the behaviors of an EM telemetry system with oil based mud (OBM) is quite different from that of EM telemetry with water based mud (WBM). In this study we will limit our discussion to only WBM scenarios.

In the second case we assume the resistivity of background formation is 10 ohm-m, and a more conductive layer with resistivity as 0.1 ohm-m exists between the downhole source and the surface receiver. The true vertical depth (TVD) of drill bit is 8000 ft, and the downhole source is 200 ft behind the bit. The TVD of upper and lower boundaries of the conductive layer are 3900 ft and 4100 ft, respectively. Operating frequency is set as 10 Hz. Fig. 5 shows the simulated current flow along the drill pipe. We can see that there is a steep descent of current magnitude within the conductive layer, and this is because the current leaks faster into this layer than in the more resistive background formation. In Fig. 6 we assume the thickness of the layer is 200 ft, and plot the strength of telemetry signal w.r.t. different resistivity of the layer. In Fig. 7 we fix the resistivity of the layer as 0.1 ohm-m but change its thickness, and calculate the corresponding received signal. From these two figures we can see that the telemetry signal will be greatly weakened if it encounters a conductive layer during the propagation from downhole source to the surface, and this is a limitation of the electromagnetic telemetry compared with mud pulse technique. In an improved electromagnetic telemetry system recently developed, one terminal of the receiver is be extended to the bottom of casing string and connected to the casing shoe instead of a point on the surface (Chen et al., 2015). Conductive layers between casing shoe and surface can be skipped in this novel design, and the picked up telemetry signal will be enhanced.

The third example is a field job done in Oklahoma. Water based drilling fluid with 1 ohm-m resistivity was used in this case. The

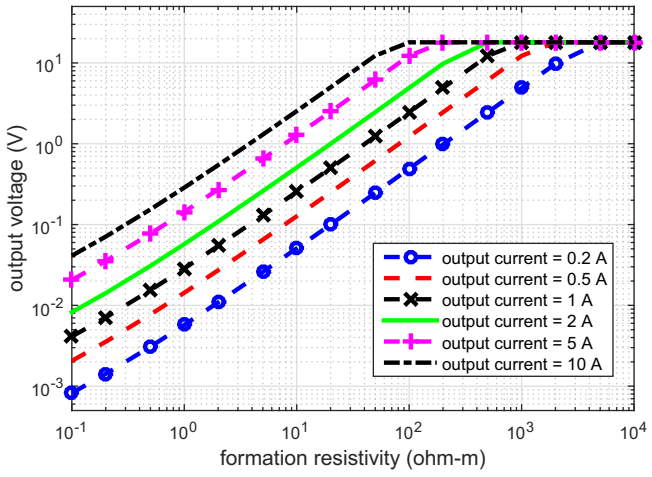

Fig. 4. The output voltage of a constant current downhole source w.r.t. underground formation resistivity. The maximum output voltage in this case is set as 18V.

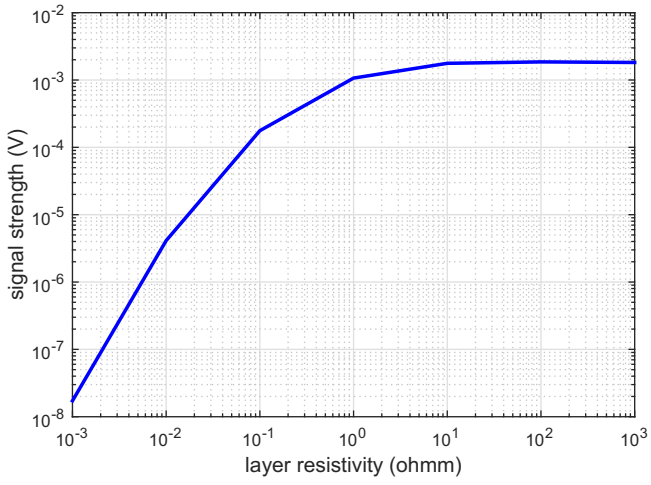

Fig. 6. Telemetry signals w.r.t. resistivity of a 200ft thick layer between bit and surface.

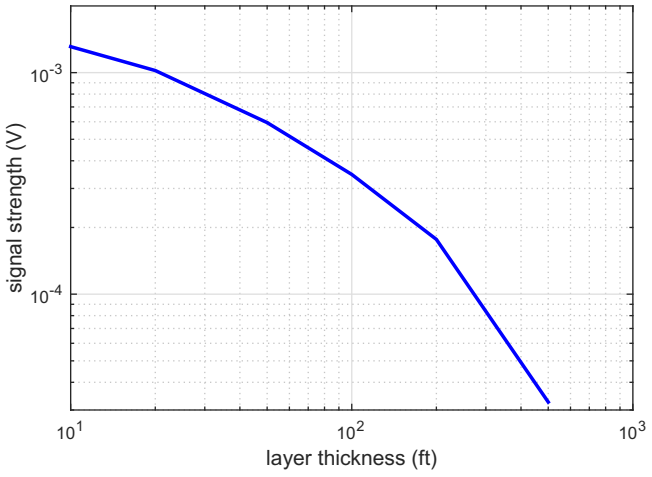

Fig. 7. Telemetry signals w.r.t. thickness of a 0.1ohm-m layer between bit and surface.

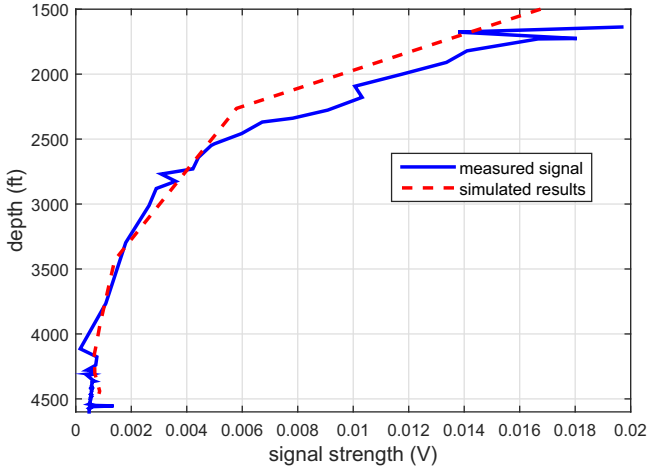

Fig. 9. Measured and simulated telemetry signals of a field case conducted in Oklahoma.

working frequency and output current of the downhole source were set as 5.33 Hz and 1 A, respectively. The diameters of drill pipe and of the borehole are 6.75 in. and 11 in., respectively. Fig. 8 shows the resistivity log and noise record of this job from 1500 ft to 4500 ft. The measured telemetry signal and simulated results are shown in Fig. 9, from which we can see that the calculated strength of EM telemetry signal follows well with the trends of the field measurements in a large range of depth. It should be noted that a lot of uncertainties in real cases will lead to discrepancies between numerical simulation results and actual measurements. For example, the resistivity distribution near the surface is subject to great variation due to temperature and moisture; the mud resistivity in borehole may change with depth; and the formation resistivity may have lateral variation in each layer, leading the whole system to be a 3D structure instead of an axisymmetric problem. After all, EM telemetry is used in subsurface wireless communication, not as a quantitative well logging tool. A very high level of accuracy may not be the first priority for modeling of EM telemetry, but an efficiently simulation method as proposed in this paper will greatly help the evaluation and decision-making of EM telemetry technique for specific field jobs.

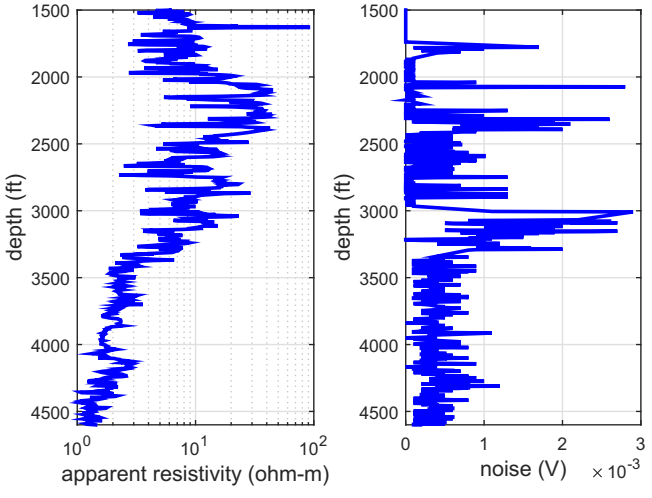

Fig. 8. (left) Resistivity log of a wireline survey in Oklahoma; (right) recorded noise during EM telemetry measurement.

5. Conclusion

An axisymmetric semianalytical finite element method for rapid simulations of electromagnetic telemetry in layered underground formation has been developed and described in the paper. Numerical examples including a homogeneous formation and a layered formation suggest that the proposed method is much more efficient than conventional finite element method. A field case was also given showing that the calculated results by the proposed method agree with measured data. It is believed that efficient simulations by the semianalytical FEM proposed in this paper will greatly facilitate the feasibility study, deployment, and optimization of an electromagnetic system for real field jobs.

References

Carcione, J.M., Poletto, F., 2002. A telegrapher equation for electric-telemetering in drill strings. IEEE Trans. Geosci. Remote Sens. 40 (5), 1047–1053.
Chen, J., 2015a. An efficient discontinuous Galerkin finite element method with nested domain decomposition for simulations of microresistivity imaging. J. Appl. Geophys. 114, 116–122.
Chen, J., 2015b. A semianalytical finite element analysis of electromagnetic propagation in stratified media. Microw. Opt. Technol. Lett. 57 (1), 15–18.
Chen, J., Li, S., MacMillan, C., Cortes, G., Wood, D., et al. 2015. Long range electromagnetic telemetry using an innovative casing antenna system. SPE Annual Technical Conference and Exhibition.
Chen, J., Tobon, L.E., Chai, M., Mix, J.A., Liu, Q.H., 2011a. Efficient implicit-explicit time stepping scheme with domain decomposition for multiscale modeling of layered structures. IEEE Trans. Compon. Packag. Manuf. Technol. 1 (9), 1438–1446.
Chen, J., Zhu, B., Zhong, W., Liu, Q.H., 2011b. A semianalytical spectral element method for the analysis of 3-d layered structures. IEEE Trans. Microwave Theory Tech. 59 (1), 1–8.
DeGauque, P., Grudzinski, R., et al. 1987. Propagation of electromagnetic waves along a drillstring of finite conductivity. SPE Drill. Eng. 2 (02), 127–134.
Maglione, R., Burban, B., Soulier, L., et al. 1994. Electromagnetic transmission improvements applied to on/offshore drilling in the Mediterranean area.
Meurant, G., 1992. A review on the inverse of symmetric tridiagonal and block tridiagonal matrices. SIAM J. Matrix Anal. Appl. 13 (3), 707–728.
Soulier, L., Lemaitre, M., et al. 1993. E.M. MWD data transmission status and perspectives. SPE/IADC Drilling Conference. Society of Petroleum Engineers
Trofimenkoff, F.N., Segal, M., Klassen, A., Haslett, J.W., 2000. Characterization of EM downhole-to-surface communication links. IEEE Trans. Geosci. Remote Sens. 38 (6), 2539–2548.
Vong, P.K., Rodger, D., Marshall, A., 2005. Modeling an electromagnetic telemetry system for signal transmission in oil fields. IEEE Trans. Magn. 41 (5), 2008–2011.
Xia, M., Chen, Z., 1993. Attenuation predictions at extremely low frequencies for measurement-while-drilling electromagnetic telemetry system. IEEE Trans. Geosci. Remote Sens. 31 (6), 1222–1228.
Zhong, W.-X., 2004. On precise integration method. J. Comput. Appl. Math. 163 (1), 59–78.
Zhong, W.-X., 2006. Duality System in Applied Mechanics and Optimal Control. vol. 5. Springer Science & Business Media.